

Outer synchronization of coupled discrete-time networks

Changpin Li,¹ Congxiang Xu,¹ Weigang Sun,² Jian Xu,³ and Jürgen Kurths⁴

¹Department of Mathematics, Shanghai University, Shanghai, China

²The School of Science, Hangzhou Dianzi University, Hangzhou, China

³Department of Engineering Mechanics and Technology, Tongji University, Shanghai, China

⁴Institute of Physics, Humboldt University, Berlin, Germany and Potsdam Institute for Climate Impact Research, Potsdam, Germany

(Received 12 September 2008; accepted 17 December 2008; published online 29 January 2009)

In this paper, synchronization between two discrete-time networks, called “outer synchronization” for brevity, is theoretically and numerically studied. First, a sufficient criterion for this outer synchronization between two coupled discrete-time networks which have the same connection topologies is derived analytically. Numerical examples are also given and they are in line with the theoretical analysis. Additionally, numerical investigations of two coupled networks which have different connection topologies are analyzed as well. The involved numerical results show that these coupled networks with different connection matrices can reach synchronization.

© 2009 American Institute of Physics. [DOI: 10.1063/1.3068357]

Synchronization inside a coupled network with/without time delays, or called “inner synchronization” for convenience, has been recently intensively and extensively studied.¹ Roughly speaking, inner synchronization inside a network, constituted by numbers of identical nodes, indicates that each node of the network approaches an asymptotical steady state. Obviously, this kind of synchronization reflects one aspect of the real world. In effect, there exist other kinds of network synchronization in the world, for example, “outer synchronization,” i.e., synchronization between two coupled networks. An outstanding example is the Acquired Immune Deficiency Syndrome, AIDS for brief,² which was originally infected among gorillas, afterwards was contagious to human beings unexpectedly. This fatal infectious disease is spread between two different mammalian communities: gorillas and human beings. People can still recall mad cow disease.³ Cows and human beings can also be regarded as two different networks in terms of network language. There are two more recent examples of coupled species: avian influenza (bird flu),⁴ and severe acute respiratory syndrome, or SARS for brevity.⁵ These cited examples show the strong importance and challenge to study the dynamics between different coupled networks.

I. INTRODUCTION

Synchronization inside a coupled network with/without time delays, or called “inner synchronization” for convenience, which is a hot topic, has been recently intensively and extensively studied.¹ This kind of synchronization reveals one aspect of the real world.⁶ In reality, synchronization between two coupled networks, or “outer synchronization”⁷ (by the way, the first paper of this reference is an early work in this respect, where two identical oscillators can be regarded as two networks; whilst the second paper is the early paper where “outer synchronization” was clearly proposed), always does exist in our lives. For

example, the infectious diseases, such as AIDS, mad cow disease, bird flu, SARS, were originally spread between two communities (or networks). This means that to study the dynamics between two coupled networks is necessary and important.

Li *et al.* have studied the synchronization between two coupled continuous-time networks, where a synchronization criterion and numerical simulations were presented.⁷ Shortly after, Li *et al.* and Tang *et al.*, further studied outer synchronization.⁸ All these studies are for continuous-time networks. In this article, we focus on studying the discrete-time case. The outline of the rest of the paper will be organized in the following. Theoretical analysis is derived in Sec. II. The illustrated examples are given in Sec. III. And the last section includes comments and conclusions.

II. THEORETICAL ANALYSIS

Throughout this paper, the following notations always work. (1) \mathbb{R} denotes the real numbers. For $u \in \mathbb{R}^n$, u^T denotes its transpose. $M \in \mathbb{R}^{n \times n}$ denotes a matrix of order n ; (2) I denotes an identity matrix; (3) $M > 0$ means that M is positive definite.

The coupled equations of two discrete-time networks can be expressed as follows:

$$x_i(t+1) = f[x_i(t)] + c \sum_{j=1}^N a_{ij} \Gamma x_j(t) + C_{YX}(Y, X), \quad (1)$$

$$y_i(t+1) = g[y_i(t)] + c \sum_{j=1}^N b_{ij} \Gamma y_j(t) + C_{XY}(X, Y), \quad (2)$$

where $c > 0$ is the coupling strength of the network, $x_i, y_i \in \mathbb{R}^n$, $i=1, 2, \dots, N$, $f, g: \mathbb{R}^n \rightarrow \mathbb{R}^n$ are continuously differentiable functions which determine the dynamical behavior of the nodes in networks X and Y , respectively. $\Gamma \in \mathbb{R}^{n \times n}$ is a constant 0-1 matrix linking coupled variables. For simplicity,

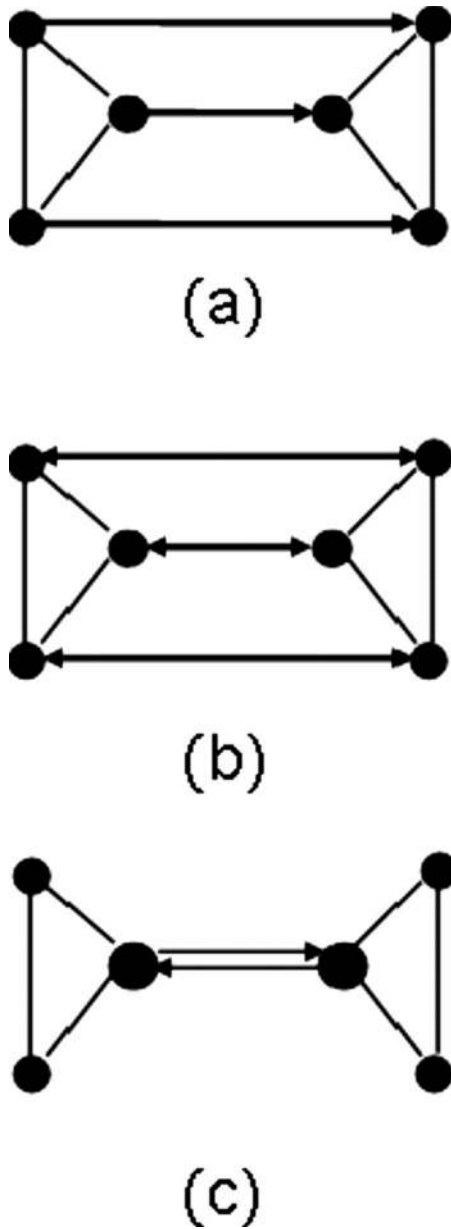


FIG. 1. Examples of actions (denoted by arrows) between two networks. (a) Unidirectional action; (b) bidirectional action; (c) special node interaction.

one often assumes that $\Gamma = \text{diag}(r_1, r_2, \dots, r_n) \geq 0$ is a diagonal matrix. $A = (a_{ij})_{N \times N}$ and $B = (b_{ij})_{N \times N}$ represent the coupling configurations of both networks, whose entries a_{ij} and b_{ij} are defined as follows: if there is a connection between node i and node j ($j \neq i$), then set $a_{ij} > 0$ and $b_{ij} > 0$, otherwise $a_{ij} = 0$, $b_{ij} = 0$ ($j \neq i$); the matrices A and B can be symmetric or asymmetric, as usual, each line sum of A and B is assumed to be zero. $C_{XY}(X, Y)$ ($C_{YX}(Y, X)$) represents the interaction from network X (Y) to network Y (X). There are lots of active forms between networks, for instance, Fig. 1 gives the actions between 3-nodes networks.

In this paper, we only study unidirectional coupling between networks (1) and (2). Here we choose $C_{XY}(X, Y) = [H - \partial f(x_i) / \partial x_i][y_i(t) - x_i(t)]$ and $C_{YX}(X, Y) = 0$, where $H \in \mathbb{R}^{n \times n}$ is a constant matrix to be set. This chosen interaction is based on the open-plus-closed-loop (OPCL) method.⁹ It is

known that the closed-loop (or “feedback”) and open-loop control methods each have their advantages and disadvantages. To overcome their shortcomings, Jackson and Grosu first combined these two methods to derive a new control method (OPCL method) and applied to complex dynamical systems; for details, see the first paper of Ref. 9. In the present paper, we use the OPCL method to construct the following scheme for a drive-response network system:

$$x_i(t + 1) = f(x_i(t)) + c \sum_{j=1}^N a_{ij} \Gamma x_j(t), \tag{3}$$

$$y_i(t + 1) = g(y_i(t)) + c \sum_{j=1}^N b_{ij} \Gamma y_j(t) + \left(H - \frac{\partial f(x_i)}{\partial x_i} \right) (y_i(t) - x_i(t)). \tag{4}$$

Network (3) is regarded as a drive one and network (4) a response one.

Definition: Networks (3) and (4) are said to attain (complete) synchronization if

$$\lim_{t \rightarrow +\infty} \|y_i(t) - x_i(t)\| = 0, \quad i = 1, 2, \dots, N. \tag{5}$$

In the following, we start with the simple case with the synchronization between systems (3) and (4), assuming that they both have the same topological structures, i.e., $A = (a_{ij})_{N \times N} = B = (b_{ij})_{N \times N}$ (they do not need to be symmetric) and same dynamics ($f = g$).

Letting $e_i = y_i - x_i$ yields

$$e_i(t + 1) = H e_i(t) + c \sum_{j=1}^N a_{ij} \Gamma e_j(t), \quad i = 1, 2, \dots, N, \tag{6}$$

by linearizing the error system around x_i . Henceforth, Eq. (6) can be rewritten as

$$e(t + 1) = H e(t) + c \Gamma e(t) A^T, \tag{7}$$

where $e = [e_1, e_2, \dots, e_N] \in \mathbb{R}^{n \times N}$ and A^T denote the transpose of A . As is well known, the coupling matrix can be decomposed into $A^T = S J S^{-1}$, where J is a Jordan form with complex eigenvalues $\lambda \in \mathbb{C}$ and S contains the corresponding eigenvectors s . Denoting $\eta = e S$ gives

$$\eta(t + 1) = H \eta(t) + c \Gamma \eta(t) J, \tag{8}$$

by multiplying Eq. (7) from the right-hand side with S , where $J = \text{diag}(J_1, J_2, \dots, J_l)$ is a block diagonal matrix, and $J_k \in \mathbb{R}^{N_k \times N_k}$ is the block corresponding to the N_k multiple eigenvalue λ_k of A , that is,

$$J = \begin{bmatrix} J_1 & & \\ & \ddots & \\ & & J_l \end{bmatrix}, \quad J_k = \begin{bmatrix} \lambda_k & 1 & 0 & \cdots & 0 \\ 0 & \lambda_k & 1 & \cdots & 0 \\ \vdots & \vdots & \ddots & \ddots & \vdots \\ 0 & 0 & \cdots & \lambda_k & 1 \\ 0 & 0 & \cdots & 0 & \lambda_k \end{bmatrix}, \tag{9}$$

$k = 1, \dots, l.$

Let $\eta = [\eta_1, \eta_2, \dots, \eta_l]$ and $\eta_k = [\eta_{k,1}, \eta_{k,2}, \dots, \eta_{k,N_k}]$. Since the sum of each line of the matrix A is assumed to be zero, we can assume $\lambda_1 = 0$ and $J_1 = 0$. It immediately follows that $\eta_1(t+1) = H\eta_1(t)$. Its zero solution is asymptotically stable if $H^T H - I$ is negative definite where I is the identity matrix. Now we rewrite Eq. (8) in component form,

$$\begin{aligned} \eta_{k,1}(t+1) &= (H + c\lambda_k \Gamma) \eta_{k,1}(t), \\ \eta_{k,p+1}(t+1) &= (H + c\lambda_k \Gamma) \eta_{k,p+1}(t) + c\Gamma \eta_{k,p}(t), \\ 1 \leq p \leq N_k - 1, \end{aligned} \tag{10a}$$

where $k=2, 3, \dots, l$.

For the first system of Eq. (10a), its zero solution is asymptotically stable if there exists a matrix $H \in \mathbb{R}^{n \times n}$ such that $P_k^T P_k - I$ are negative definite, where

$$P_k = \begin{bmatrix} H + c\alpha_k \Gamma & -c\beta_k \Gamma \\ c\beta_k \Gamma & H + c\alpha_k \Gamma \end{bmatrix}, \quad k = 2, \dots, l. \tag{10b}$$

For the second system of Eq. (10a), its zero solution is asymptotically stable if $Q_k^T Q_k - I$ are negative definite, in which

$$Q_k = \text{diag}(c\Gamma, c\Gamma, P_k), \quad k = 2, \dots, l. \tag{10c}$$

The proofs are given in the Appendix.

So we can assert the

Synchronization Criterion I if (a) $A=B$, and each line sum of them is zero; (b) $f=g$; and (c) $H^T H - I$, $P_k^T P_k - I$, $Q_k^T Q_k - I$, $k=2, \dots, l$, are negative definite, in which P_k and Q_k are given in Eqs. (10b) and (10c), respectively, then networks (3) and (4) can be synchronized.

If we set $L_A(X) = c(A \otimes \Gamma)X$, $L_B(Y) = c(B \otimes \Gamma)Y$, where \otimes denotes the Kronecker product, $f(x_i) \rightarrow f_i(x_i)$ in Eqs. (3) and (4), $g(y_i) \rightarrow f_i(y_i)$, $H \rightarrow H_i$ in Eq. (4), then Eqs. (3) and (4) can be rewritten in a compact form

$$X(t+1) = F(X(t)) + L_A(X(t)), \tag{11}$$

$$Y(t+1) = F(Y(t)) + L_B(Y(t)) + \left(\Lambda - \frac{\partial F(X)}{\partial X} \right) (Y(t) - X(t)), \tag{12}$$

where $X = (x_1^T, \dots, x_N^T)^T$, $Y = (y_1^T, \dots, y_N^T)^T \in \mathbb{R}^{nN}$, $F(X) = (f_1(x_1)^T, \dots, f_N(x_N)^T)^T$, $F(Y) = (f_1(y_1)^T, \dots, f_N(y_N)^T)^T \in \mathbb{R}^{nN}$, $\Lambda = \text{diag}(H_1, H_2, \dots, H_N)$.

If $A=B$, then the error system between Eqs. (11) and (12) reads

$$e(t+1) = (\Lambda + cA \otimes \Gamma)e(t), \tag{13}$$

in which $e = (e_1^T, e_2^T, \dots, e_N^T)^T \in \mathbb{R}^{nN}$.

Compared to the error system (13) with system (7), the former is a system of equations in \mathbb{R}^{nN} , and the latter is a matrix equation in $\mathbb{R}^{n \times N}$. From error system (13), it is immediately seen that

Synchronization Criterion II if (a) $A=B$ and (b) all the eigenvalues of $\Lambda + cA \otimes \Gamma$ lie inside the unit circle, then networks (11) and (12) can be synchronized.

Since the error systems (7) and (13) (here provided that all H_i are identical) have different expressions, the derived synchronization conditions are different. Whether or not the synchronization condition in *Synchronization Criterion I* for

networks (3) and (4) is equivalent to that in *Synchronization Criterion II* for networks (11) and (12) provided that all f_i and H_i are the same is a puzzle and remains unsolved. And we cannot make a decision which Synchronization Criterion is more convenient in analyzing outer synchronization of coupled networks.

On the other hand, *Synchronization Criteria I and II* also hold for the following bidirectional coupled networks:

$$\begin{aligned} x_i(t+1) &= f(x_i(t)) + \alpha \left(H - \frac{\partial f(x_i)}{\partial x_i} \right) (x_i(t) - y_i(t)) \\ &\quad + c \sum_{j=1}^N a_{ij} \Gamma x_j(t), \quad i = 1, 2, \dots, N, \end{aligned} \tag{14}$$

$$\begin{aligned} y_i(t+1) &= f(y_i(t)) + (1 - \alpha) \left(H - \frac{\partial f(x_i)}{\partial x_i} \right) (y_i(t) - x_i(t)) \\ &\quad + c \sum_{j=1}^N b_{ij} \Gamma y_j(t), \quad i = 1, 2, \dots, N, \end{aligned} \tag{15}$$

where α is a parameter. Here we do not further consider synchronization between two bidirectional networks. Here and throughout, we only use *Synchronization Criterion I*.

If networks (3) and (4) [or Eqs. (11) and (12)] have different connection topologies, i.e., $A \neq B$, then generalized synchronization¹⁰ between them often appears, but no any theoretical analysis regarding synchronization is available until now due to technical difficulties (see the reviews in Refs. 7 and 10). We hope that this puzzle can be solved in the near future. Here we will also present numerical studies for the case with $A \neq B$ in the following.

Next we do some numerical experiments. In the drive-response networks (3) and (4), the node systems are chosen as the one-dimensional Logistic map and the two-dimensional Hénon map.

III. ILLUSTRATIVE EXAMPLES

The logistic map

$$x(t+1) = \mu x(t)(1 - x(t)), \tag{16}$$

has μ as the adjustable parameter. The Hénon map is as follows:

$$x(t+1) = 1 + y(t) - ax^2(t), \quad y(t+1) = bx(t). \tag{17}$$

If $a=1.4$ and $b=0.3$, this two-dimensional map has a strange attractor.

Here, we always let Γ be the unit matrix for convenience. We proceed to our numerical studies for two situations: $A=B$, and $A \neq B$.

A. Equivalent topological structure, i.e., $A=B$

First, we study the situation $A=B$. Through the LMI toolbox in MATLAB, we choose (H, c) , (i) generate A which has the small-world network property¹¹ (this case is that A is symmetric), then let $B=A$; (ii) generate A at random which makes the network (3) directed (this case is that A is non-symmetric), then set $B=A$. These H, c, A make the condition

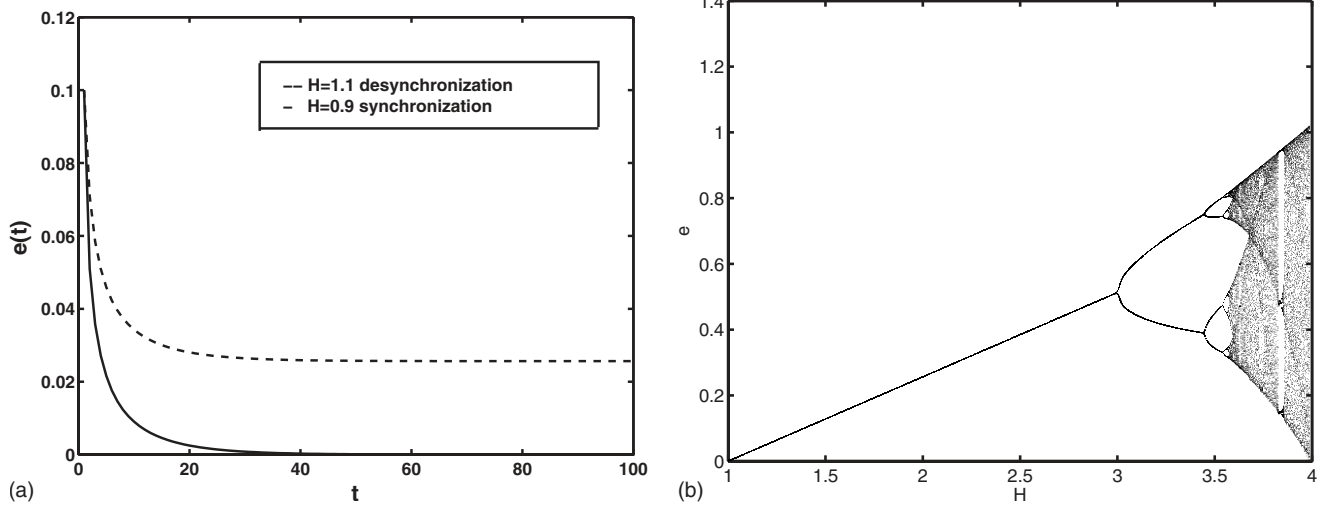


FIG. 2. Synchronization-desynchronization diagram between Eqs. (3) and (4), $c=0.001$, $\mu=3.9$, $\Gamma=1$, A with order $N=50$ ($p=0.1$, $m=3$) is generated in case (i), and $B=A$. (a) Synchronization for $H=0.9$, desynchronization for $H=1.1$. (b) Bifurcation diagram of e vs H .

of Synchronization Criterion I for networks (3) and (4) be satisfied. In the following, we study cases (i) and (ii).

(i) $A(=B)$ is symmetric. For the logistic map with $\mu=3.9$, choose (H, c) and A such that the condition of the synchronization criterion holds. Once A with order $N=50$ (the connection probability and average degree for matrix A are chosen as $p=0.1$, $m=3$) is taken, using the LMI toolbox in MATLAB, we find (H, c) such that the condition of the synchronization criterion is satisfied, e.g., if $H=0$, then $c \in (0, 0.007)$; if $c=0.001$, then $-1 < H < 1$, for this value c , Eqs. (3) and (4) cannot be synchronized if $|H| > 1$. In Fig. 2(a), when $H=0.9$, networks (3) and (4) can be synchronized but they cannot be synchronized when $H=1.1$, where $c=0.001$, $\mu=3.9$, and $\|e(t)\| = \max_{1 \leq i \leq 50} |y_i(t) - x_i(t)|$. Although desynchronization happens for this case with $c=0.001$ and $H > 1$ (the case $H < -1$ is omitted here), the error of each

node is dramatically stabilized to nonzero constant(s), denoted as e , when t approaches $+\infty$, and interesting bifurcations appear. In Fig. 2(b), the bifurcation diagram for e in dependence on H is displayed.

Furthermore, we investigate the relationships among the network size N , the average degree m of the network are the connection probability p which are used in generating the network, and the maximum coupling strength c available for synchronization. We fix the network size $N=1000$ and $\mu=3.9$, $\Gamma=1$. We find that the maximum coupling strength c decreases with the increase of the average degree m for fixed p , see Fig. 3(a). Next, we fix $\mu=3.9$, $\Gamma=1$, $p=0.1$. We find that the maximum coupling strength c decreases with the increase of network size N for the fixed $m(\leq 20)$, see Fig. 3(b).

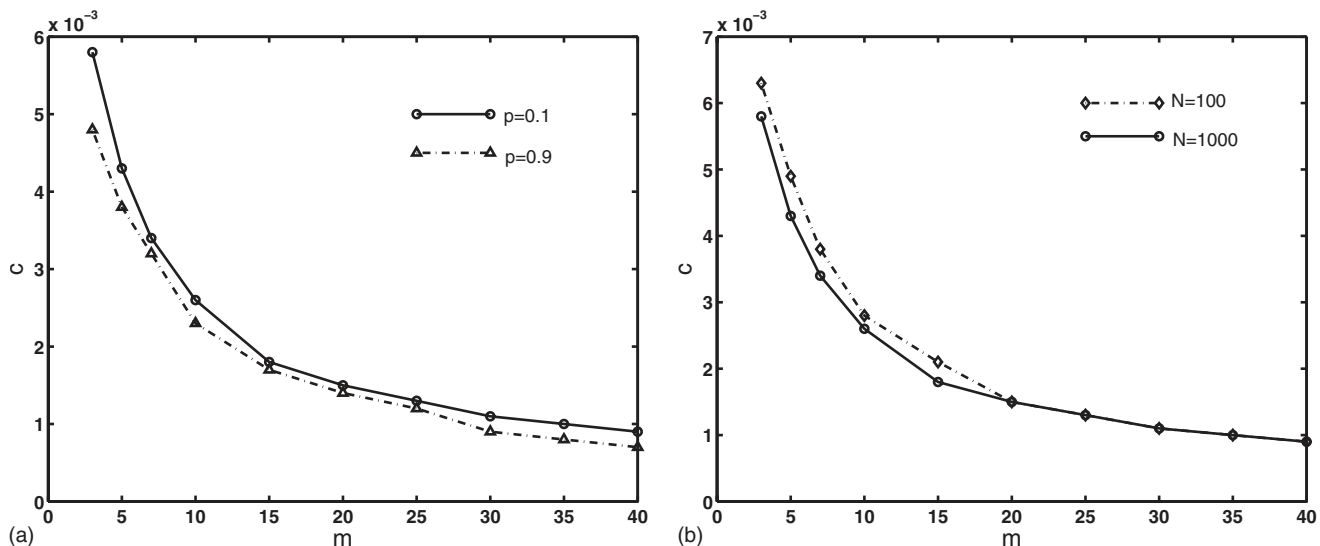


FIG. 3. Relation diagram among the network size N , the average degree m , the connection probability p , and the maximum coupling strength c , where $\mu=3.9$, $\Gamma=1$, A is generated in case (i), and $B=A$. (a) The maximum coupling strength c available in dependence on the average degree m of matrix A with $N=1000$ for different connection probability $p=0.1$ and $p=0.9$. (b) The maximum coupling strength c available in dependence on the average degree m of matrix A with order $N=100$ and $N=1000$ for fixed $p=0.1$.

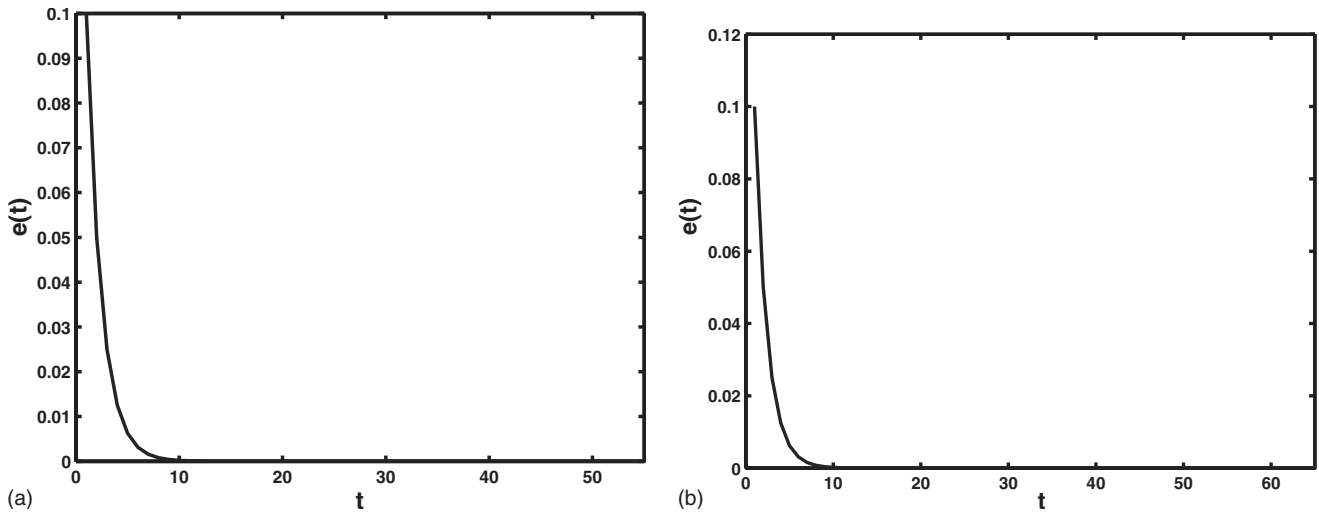


FIG. 4. Synchronization diagrams for case (iii), where A is chosen as that in case (i) and B is chosen as that in case (ii), $c=0.000009$. (a) The node system is the logistic map. (b) The node system is the Hénon map.

For the Hénon map (17) with $a=1.4$ and $b=0.3$, we take the same A used in Fig. 1, $B=A$, $\Gamma=\text{diag}(1, 1)$. By almost the same procedure, we can get (H, c) such that the condition of the synchronization criterion holds. In our numerical studies, if we choose $H=\text{diag}(0.5, 0.5)$ for brevity, we find when $c \in (0, 0.001)$ such that networks (3) and (4) can achieve synchronization. The corresponding figures are omitted here.

Next, we study case (ii).

(ii) $A(=B)$ is asymmetric. We generate A with order $N=50$ randomly which makes the network (3) directed (this case is that A is nonsymmetric), and set $B=A$. In networks (3) and (4), we let Γ be the identity matrix and H be a zero matrix. If we choose Eq. (16) with $\mu=3.9$ and Eq. (17) with $a=1.4$, $b=0.3$ as node systems in networks (3) and (4), we find that Eqs. (3) and (4) can be synchronized when the coupling strengths c lie in $(0, 0.002)$ and $(0, 10^{-4})$, respectively. By comparing cases (i) and (ii), we find that the coupling strength c relates to the connection matrix A for the situation $A=B$ under suitable conditions, i.e., the maximum coupling strength value c concerning synchronization between Eqs. (3) and (4) for symmetric matrix A is larger than that for the nonsymmetric matrix A . The associate figures are also left out here.

B. Different topological structure, i.e., $A \neq B$

Although the synchronization criterion is not derived for the case $A \neq B$, i.e., the drive network (3) and the response one (4) have different connection topologies. However, we can still numerically study the coupled networks (3) and (4). The case $A \neq B$ can be divided into four subcases: (iii) A is symmetric but B is not; (iv) B is symmetric but A is not; (v) A, B are both symmetric but they are not equal; (vi) A, B are both nonsymmetric and they are not equal. By numerical simulations, we indeed observe synchronization between Eqs. (3) and (4). If A is chosen as that in case (i) and B is chosen as that in case (ii); B is chosen as that in case (i) and

A is chosen as that in case (ii); A, B are chosen as those in case (i) but they are not equal; A, B are chosen as those in case (ii) but they are not equal. Set still H be a zero matrix for convenience. The networks (3) and (4) with node systems (16) with $\mu=3.9$ and Eq. (17) with $a=1.4$, $b=0.3$ can reach synchronization. For the logistic map with $\mu=3.9$, the coupling strength c lies in $(0, 10^{-5})$ in (iii), $(0, 10^{-5})$ in (iv), $(0, 10^{-4})$ in (v) and $(0, 10^{-4})$ in (vi). For the Hénon map, the coupling strength c lies in $(0, 10^{-5})$ in cases (iii)–(vi). Here we only present the synchronization diagrams for case (iii), see Fig. 4. From numerical simulations, one can see that the synchronization interval regarding c for networks (3) and (4) in situation $A \neq B$ is narrower than that in $A=B$.

IV. COMMENTS AND CONCLUSIONS

In this paper, outer synchronization between two coupled discrete-time networks is theoretically and numerically studied. If networks (3) and (4), or the more general case (11) and (12), have the same topological connections, i.e., $A=B$, then a theoretical analysis on synchronization between them is derived. Numerical examples are also given, which fit the analytical results. From our numerical simulations, we can especially see that the maximum coupling strength c has relations to the symmetric properties of matrices A and B . In detail, the maximum coupling strength value c of the case with symmetric matrices $A=B$ is larger than that for the case with nonsymmetric ones $A=B$. If $A \neq B$, such a value c is the smallest, nearly equal to zero.

Besides, the scale-free network¹² generally has a small-world property,¹¹ so we investigate here only two coupled small-world networks by numerical calculations. From our numerical computations available, we can see that the maximum coupling strength value c for synchronization relates also to the network size N , linking the probability p and the average degree m . Through the numerical experiments, we

find that (1) the maximum coupling strength value c decreases with increasing average degree m for the fixed linking probability p and the networks size N . (2) Such a value c decreases with the increase of the average degree p for the given average degree m and the network size N . (3) This maximum value c decreases with the increase of network size N for the known average degree m and linking probability p .

Although outer synchronization between coupled networks, which is different from the intranetwork synchronization, exists in our lives, and such a (de)synchronization has potential applications in the real world, and studies on such synchronization between coupled networks are very limited. We hope that the investigation and studies in this regard will appear elsewhere.

ACKNOWLEDGMENTS

The authors wish to thank two anonymous reviewers for their careful reading and providing beneficial correction suggestions. This work was partially supported by the National Natural Science Foundation under Grant No. 10872119, Shanghai Leading Academic Discipline Project under Grant No. J50101, Key Disciplines of Shanghai Municipality under Grant No. S30104, Systems Biology Research Foundation of Shanghai University, SFB 555 (DFG) and EC project BRACCIA Contract No. 517133 NEST.

APPENDIX: THE PROOF OF STABILITY OF ZERO SOLUTION TO SYSTEM (10a)

Now we study the stability of the zero solution, i.e., the synchronized regime, of system (10a).

Let $\lambda_k = \alpha_k + i\beta_k$, $\eta_{k,1} = u_{k,1} + iv_{k,1}$, where i is the imaginary unit, $\alpha_k, \beta_k \in \mathbb{R}, u_{k,1}, v_{k,1} \in \mathbb{R}^n$. Then the first equation of (10a) can be decomposed into

$$u_{k,1}(t+1) = (H + c\alpha_k\Gamma)u_{k,1}(t) - c\beta_k\Gamma v_{k,1}(t),$$

$$v_{k,1}(t+1) = (H + c\alpha_k\Gamma)v_{k,1}(t) + c\beta_k\Gamma u_{k,1}(t).$$

Here, we construct the Lyapunov function as the following form:

$$V(t) = u_{k,1}^T(t)u_{k,1}(t) + v_{k,1}^T(t)v_{k,1}(t).$$

Therefore we get

$$\begin{aligned} \Delta V(t) &= V(t+1) - V(t) \\ &= \begin{bmatrix} u(t) \\ v(t) \end{bmatrix}^T \begin{bmatrix} H + c\alpha_k\Gamma & -c\beta_k\Gamma \\ c\beta_k\Gamma & H + c\alpha_k\Gamma \end{bmatrix}^T \\ &\quad \times \begin{bmatrix} H + c\alpha_k\Gamma & -c\beta_k\Gamma \\ c\beta_k\Gamma & H + c\alpha_k\Gamma \end{bmatrix} \begin{bmatrix} u(t) \\ v(t) \end{bmatrix} - \begin{bmatrix} u(t) \\ v(t) \end{bmatrix}^T \begin{bmatrix} u(t) \\ v(t) \end{bmatrix} \\ &= [u(t) \quad v(t)][P_k^T P_k - I][u(t) \quad v(t)]^T, \end{aligned}$$

where

$$P_k = \begin{bmatrix} H + c\alpha_k\Gamma & -c\beta_k\Gamma \\ c\beta_k\Gamma & H + c\alpha_k\Gamma \end{bmatrix}, \quad k = 2, \dots, l. \tag{A1}$$

If there exists a matrix $H \in \mathbb{R}^{n \times n}$ such that $P_k^T P_k - I$ are negative definite, then the zero solution of the first system of Eq. (10a) is asymptotically stable.

Next, define $\eta_{k,p+1} = u_{k,p+1} + iv_{k,p+1}$, the second system of Eq. (10a) reads as

$$\begin{aligned} u_{k,p+1}(t+1) &= (H + c\alpha_k\Gamma)u_{k,p+1}(t) - c\beta_k\Gamma v_{k,p+1}(t) \\ &\quad + c\Gamma u_{k,p}(t), \quad 1 \leq p \leq N_k - 1, \end{aligned}$$

$$\begin{aligned} v_{k,p+1}(t+1) &= (H + c\alpha_k\Gamma)v_{k,p+1}(t) + c\beta_k\Gamma u_{k,p+1}(t) \\ &\quad + c\Gamma v_{k,p}(t), \quad 1 \leq p \leq N_k - 1. \end{aligned}$$

Choose the Lyapunov function as

$$\begin{aligned} \bar{V}(t) &= u_{k,p}^T(t)u_{k,p}(t) + v_{k,p}^T(t)v_{k,p}(t) + u_{k,p+1}^T(t)u_{k,p+1}(t) \\ &\quad + v_{k,p+1}^T(t)v_{k,p+1}(t), \end{aligned}$$

therefore,

$$\begin{aligned} \Delta \bar{V}(t) &= \bar{V}(t+1, u(t+1)) - \bar{V}(t, u(t)) \\ &= \begin{bmatrix} u_{k,p}(t) \\ v_{k,p}(t) \\ u_{k,p+1}(t) \\ v_{k,p+1}(t) \end{bmatrix}^T \begin{bmatrix} c\Gamma & 0 & 0 & 0 \\ 0 & c\Gamma & 0 & 0 \\ 0 & 0 & H + c\alpha_k\Gamma & -c\beta_k\Gamma \\ 0 & 0 & c\beta_k\Gamma & H + c\alpha_k\Gamma \end{bmatrix}^T \begin{bmatrix} c\Gamma & 0 & 0 & 0 \\ 0 & c\Gamma & 0 & 0 \\ 0 & 0 & H + c\alpha_k\Gamma & -c\beta_k\Gamma \\ 0 & 0 & c\beta_k\Gamma & H + c\alpha_k\Gamma \end{bmatrix} \begin{bmatrix} u_{k,p}(t) \\ v_{k,p}(t) \\ u_{k,p+1}(t) \\ v_{k,p+1}(t) \end{bmatrix} \\ &\quad - \begin{bmatrix} u_{k,p}(t) \\ v_{k,p}(t) \\ u_{k,p+1}(t) \\ v_{k,p+1}(t) \end{bmatrix}^T \begin{bmatrix} u_{k,p}(t) \\ v_{k,p}(t) \\ u_{k,p+1}(t) \\ v_{k,p+1}(t) \end{bmatrix} \\ &= [u_{k,p} \quad v_{k,p} \quad u_{k,p+1} \quad v_{k,p+1}][Q_k^T Q_k - I][u_{k,p} \quad v_{k,p} \quad u_{k,p+1} \quad v_{k,p+1}]^T, \end{aligned}$$

in which

$$Q_k = \text{diag}(c\Gamma, c\Gamma, P_k), \quad k = 2, \dots, l. \tag{A2}$$

The zero solution to the second system of Eq. (10a) is asymptotically stable if $Q_k^T Q_k - I$ are negative definite.

So if $P_k^T P_k - I$ and $Q_k^T Q_k - I$, $k=2, \dots, l$, are negative definite, then the zero solution to system (10a) is asymptotically stable. The proof is thus complete.

¹S. Boccaletti, V. Latora, Y. Morento, M. Chavez, and D.-U. Hwang, *Phys. Rep.* **424**, 175 (2006); Q. Y. Wang, Q. S. Lu, and G. Chen, *Europhys. Lett.* **77**, 10004 (2007); J. Zhou, L. Xiang, and Z. Liu, *Physica A* **385**, 729 (2007); L. Huang, Y.-C. Lai, and R. A. Gatenby, *Phys. Rev. E* **77**, 016103 (2008).

²V. Berridge, *AIDS and Contemporary History* (Cambridge University Press, Cambridge, 2002).

³For mad cow disease, visit the webpage http://www.newstarget.com/mad_cow_disease.html.

⁴M. Small, D. M. Walker, and C. K. Tse, *Phys. Rev. Lett.* **99**, 188702 (2007).

⁵For SARS in details, explore http://english.peopledaily.com.cn/zhuanti/Zhuanti_335.shtml.

⁶R. Steuer, T. Gross, J. Selbig, and B. Blasius, *Proc. Natl. Acad. Sci. U.S.A.*

103, 11868 (2006); W. H. Deng, Y. J. Wu, and C. P. Li, *Comput. Math. Appl.* **54**, 671 (2007); W. G. Sun, C. X. Xu, C. P. Li, and J. Q. Fang, *Commun. Theor. Phys.* **47**, 1073 (2007); W. G. Sun, Y. Chen, C. P. Li, and J. Q. Fang, *ibid.* **48**, 871 (2007); W. G. Sun, Y. Y. Yang, C. P. Li, and J. Q. Fang, "Synchronization in delayed map lattices with scale-free interactions," *Int. J. Non-Linear Mech.* (in press).

⁷E. Montbrío, J. Kurths, and B. Blasius, *Phys. Rev. E* **70**, 056125 (2004); C. P. Li, W. G. Sun, and J. Kurths, *ibid.* **76**, 046204 (2007).

⁸Y. Li, Z. R. Liu, and J. B. Zhang, *Chin. Phys. Lett.* **25**, 874 (2008); H. Tang, L. Chen, J. Lu, and C. K. Tse, *Physica A* **387**, 5623 (2008).

⁹E. A. Jackson and I. Grosu, *Physica D* **85**, 1 (1995); A. I. Lerescu, N. Constandache, S. Oancea, and I. Grosu, *Chaos, Solitons Fractals* **22**, 599 (2004); I. Grosu, E. Padmanaban, P. K. Roy, and S. K. Dana, *Phys. Rev. Lett.* **100**, 234102 (2008).

¹⁰S. Boccaletti, J. Kurths, G. Osipov, D. L. Vauadares, and C. S. Zhou, *Phys. Rep.* **366**, 1 (2002).

¹¹D. J. Watts and S. H. Strogatz, *Nature (London)* **393**, 440 (1998).

¹²A. L. Barabási and R. Albert, *Science* **286**, 509 (1999).